iScience, Volume *24*

Supplemental information

Semaphorin3E-PlexinD1 signaling in coronary artery and lymphatic vessel development with clinical implications in myocardial recovery

Kazuaki Maruyama, Kazuaki Naemura, Yuichiro Arima, Yasunobu Uchijima, Hiroaki Nagao, Kenji Yoshihara, Manvendra K. Singh, Akiyoshi Uemura, Fumio Matsuzaki, Yutaka Yoshida, Yukiko Kurihara, Sachiko Miyagawa-Tomita, and Hiroki Kurihara

Figure S1

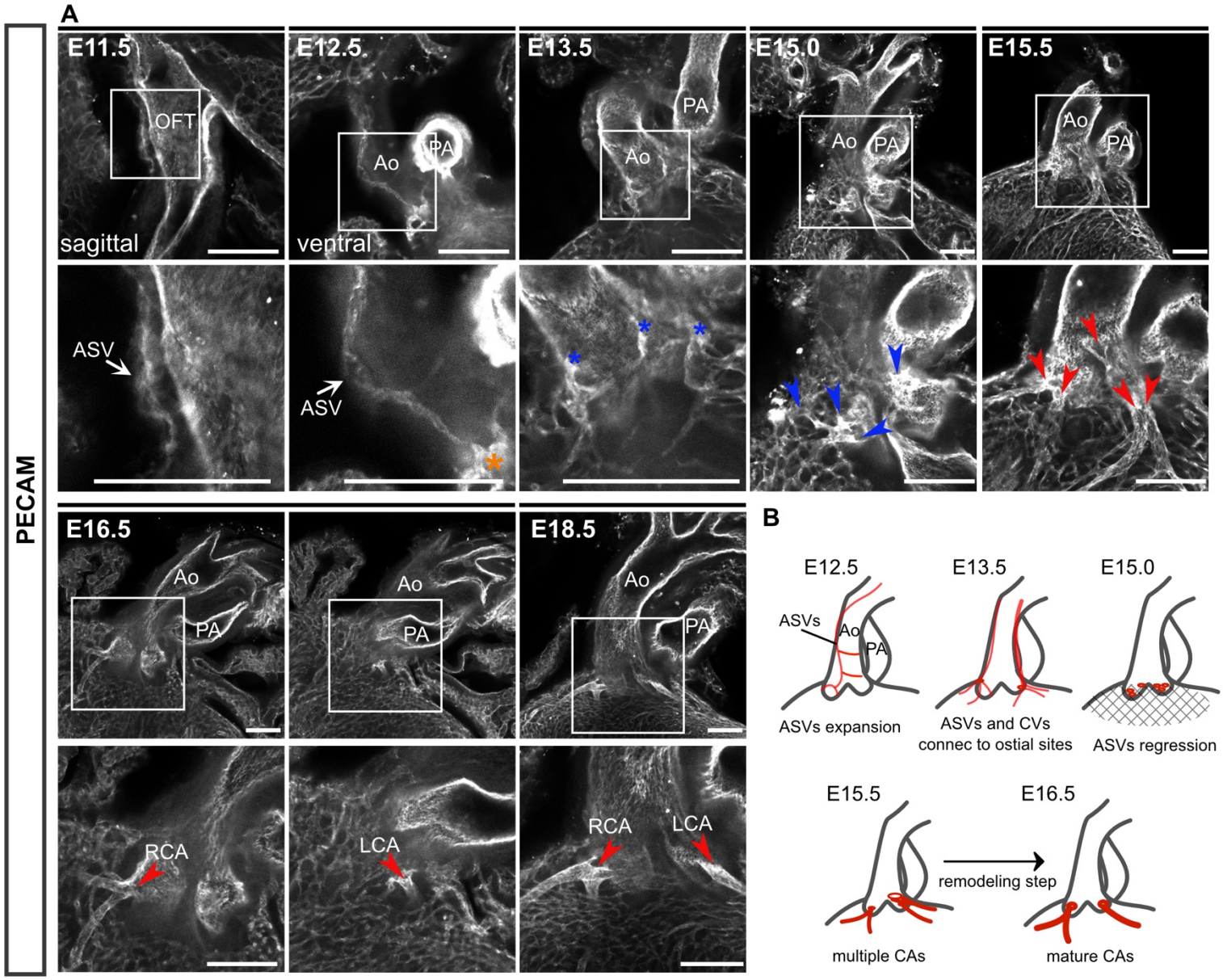
A
PECAM
E11.5
OFT
sagittal
E12.5
Ao
PA
ventral
E13.5
PA
Ao
E15.0
Ao
PA
E15.5
Ao
PA
ASV
ASV
E16.5
Ao
PA
E18.5
Ao
PA
RCA
LCA
RCA
LCA
B
E12.5
ASVs
Ao
PA
ASVs expansion
E13.5
ASVs and CVs
connec to ostial sites
E15.0
ASVs regression
E15.5
E16.5
remodeling step
multiple CAs
mature CAs

Figure S1. CA ostium development in wild type mice

(A) Whole-mount confocal images of wild type hearts labeled for PECAM. White arrows indicated ASVs. Orange asterisks indicated the ASVs connection site to the aortic lumen at E12.5. CVs grew and connected to the aortic sinuses at multiple sites (blue asterisks). These connections were increased at E15.0 (blue arrowheads). At E15.5, large connections formed between the aorta and CVs (red arrowheads). At E16.5, two mature ostia formed (red arrowheads) and maintained at E18.5 (red arrowheads). (**B**) Schematic representation of CA ostium development in wild type embryos. ASVs, aortic subepicardial vessels; CVs, coronary vessels. Ao, aorta; PA, pulmonary artery; RCA, right coronary artery; LCA, left coronary artery. Scale bars, 100 μm (**A**).

Figure S1, related to Figure 2

Figure S2

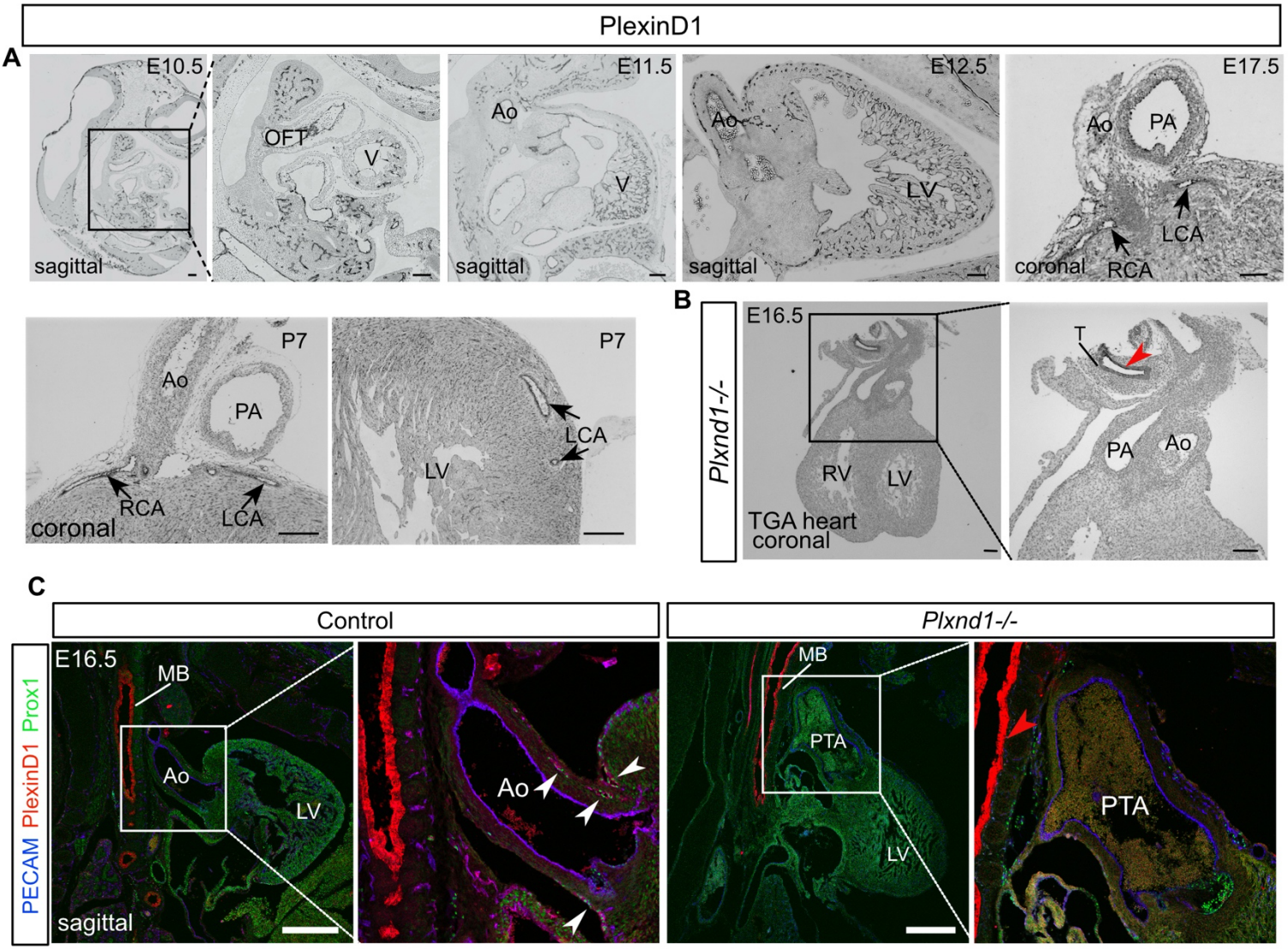
PlexinD1
A
E10.5
OFT
V
sagittal
E11.5
Ao
V
sagittal
E12.5
Ao
LV
sagittal
E17.5
Ao
PA
LCA
RCA
coronal
P7
Ao
PA
RCA
LCA
coronal
P7
LCA
LV
B
Plxnd1-/-
E16.5
RV
LV
TGA heart
coronal
T
PA
Ao
C
Control
Plxnd1-/-
PECAM PlexinD1 Prox1
E16.5
MB
Ao
LV
sagittal
Ao
MB
PTA
LV
PTA

Figure S2. PlexinD1 is expressed in blood and lymphatic endothelial cells

(A, B) Paraffin sections immunostained for PlexinD1 in the developing heart at the indicated embryonic and postnatal stages. PlexinD1 was expressed in the endocardium and the endothelium, including the CAs (black arrows). (**B**) In *Plxnd1*$^{-/-}$ hearts at E16.5, PlexinD1 was undetectable, except in the bronchial epithelium (red arrowhead). (**C**) Sagittal sections of control and *Plxnd1*$^{-/-}$ embryos labeled for PECAM, Prox1 and PlexinD1 at E16.5. PlexinD1 was detected in lymphatic vessels around the aorta and merged with PECAM and Prox1 in control embryos (white arrowheads), whereas PlexinD1 was undetectable in *Plxnd1*$^{-/-}$ embryos, except in the bronchial epithelium (red arrowhead). OFT, outflow tract; V, ventricle; Ao, aorta; LV, left ventricle; PA, pulmonary artery; RCA, right coronary artery; LCA, left coronary artery; RV, right ventricle; T, trachea; MB, main bronchus; PTA, persistent truncus arteriosus. Scale bars, 100 μm **(A, B)**, 500 μm (**C**).

Figure S2, related to Figure 3

Figure S3

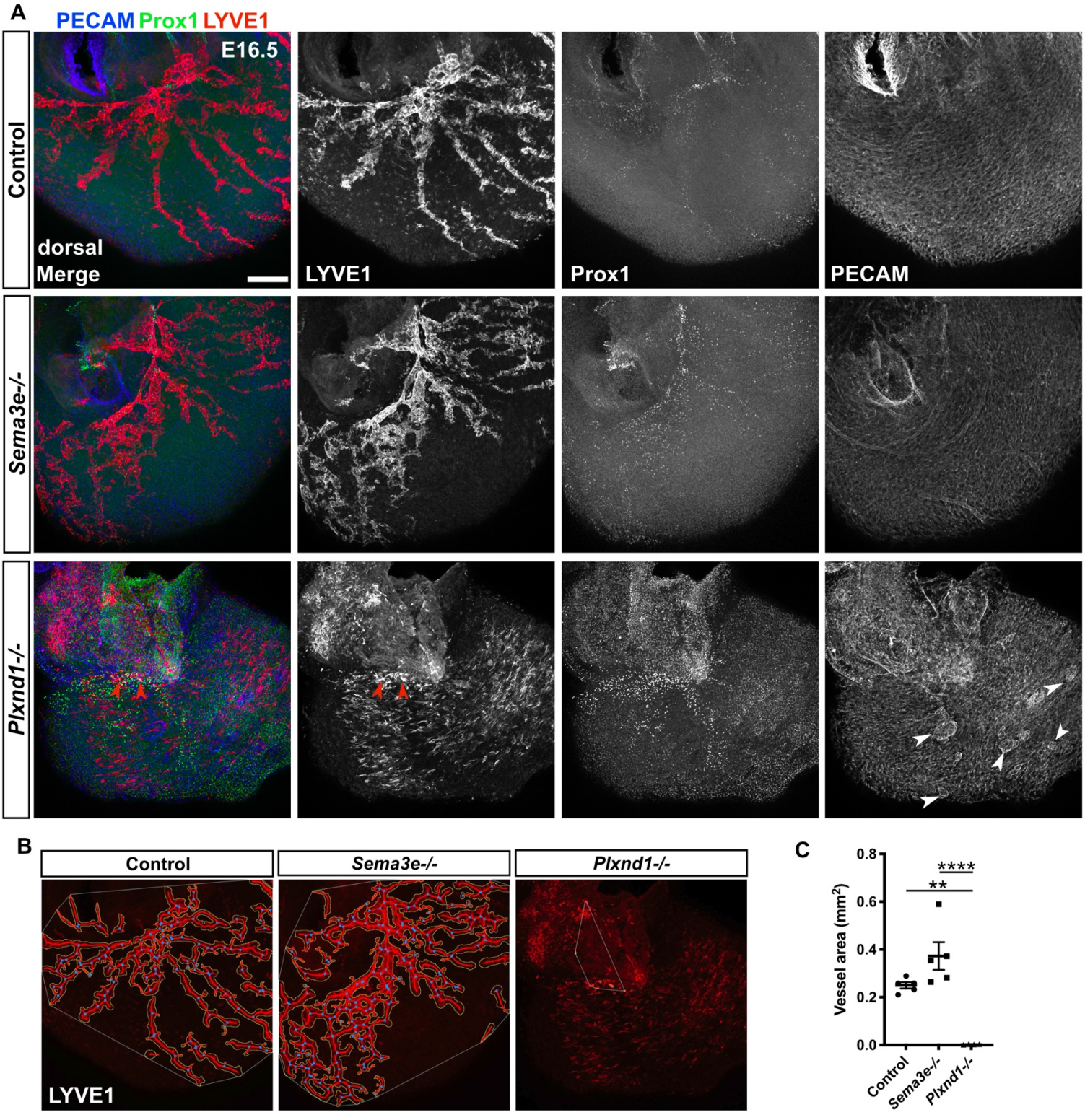
A
PECAM Prox1 LYVE1
Control
E16.5
dorsal
Merge
LYVE1
Prox1
PECAM
Sema3e-/-
Plxnd1-/-
B
Control
Sema3e-/-
Plxnd1-/-
LYVE1
C
Vessel area (mm2)
0.8
0.6
0.4
0.2
0.0
****
**
Control
Sema3e-/-
Plxnd1-/-

Figure S3. Effects of impaired Sema3E-PlexinD1 signaling on cardiac lymphatic vessel formation

(A) Whole-mount confocal images of control, *Sema3e*$^{-/-}$, or *Plxnd1*$^{-/-}$ hearts labeled for PECAM, Prox1, and LYVE1. In *Sema3e*$^{-/-}$ mice, hyperplastic PECAM^{+}/Prox1^{+}/LYVE1^{+} cardiac lymphatic vessels were observed. In contrast, PECAM^{+} ectopic CVs (white arrowheads) and Prox1^{+} lymphatic vessels with partial LYVE1 expression were observed in *Plxnd1*$^{-/-}$ mice (red arrowheads). (**B)** Whole-mount confocal images of control, *Sema3e*$^{-/-}$ or *Plxnd1*$^{-/-}$ hearts at E16.5 captured for AngioTool analyses. The tracing was depicted for LYVE1^{+} vessels (red) and branch points (blue) and enabled the quantitative assessment of vessel parameters. **(C)** Quantification of vessel area. CVs, coronary vessels. Each dot represents a value obtained from one sample. All the data are presented as the means±SEM, and statistical analyses were performed using a one-way ANOVA between groups and post hoc multiple comparisons using Bonferroni's test. * P<0.05, ** P<0.01, ****P<0.0001. Scale bars, 100 μm **(A)**.

Figure S3, related to Figure 4 and 5

Figure S4

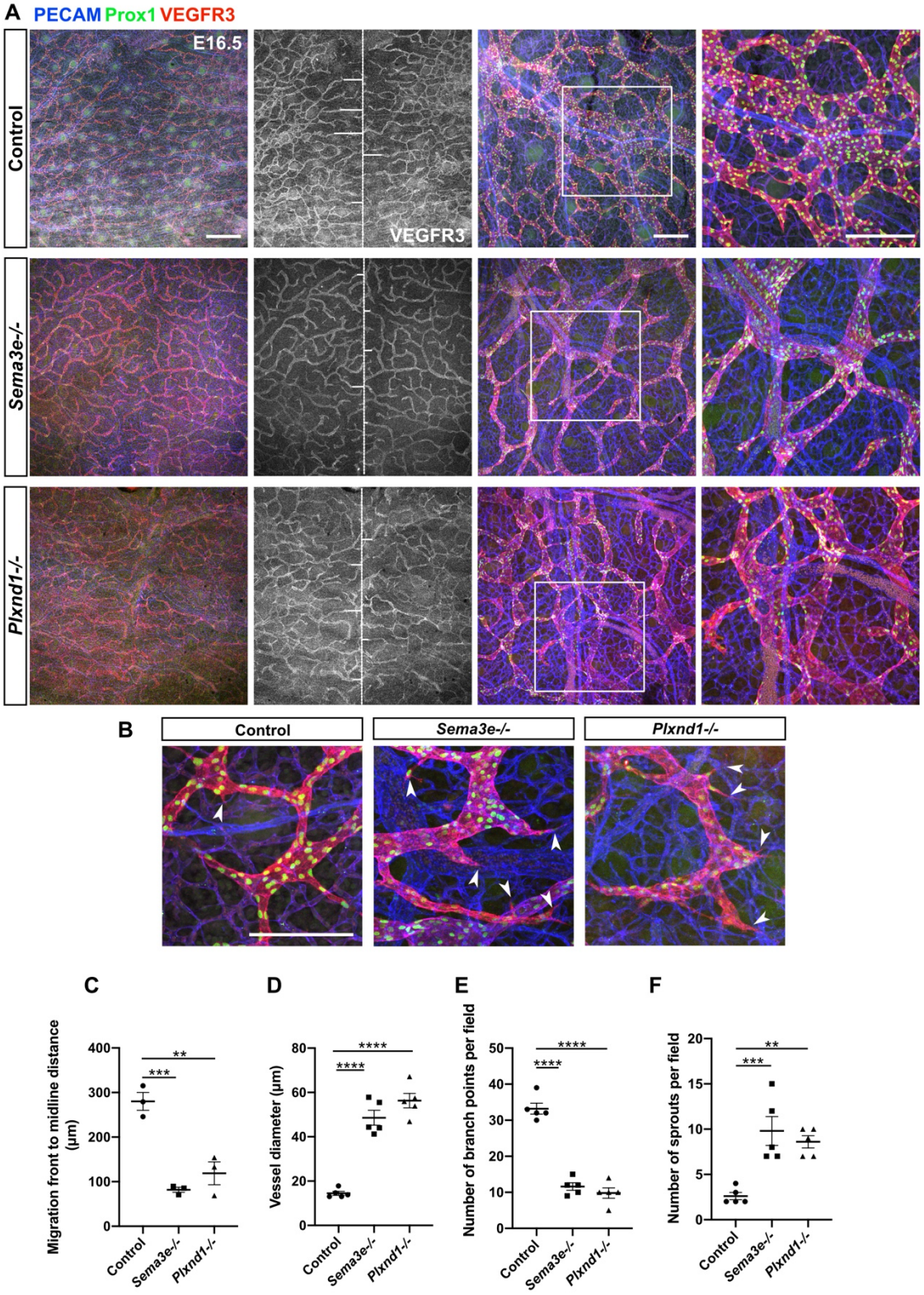
A
PECAM Prox1 VEGFR3
E16.5
Control
Sema3e-/-
Plxnd1-/-
VEGFR3
B
Control
Sema3e-/-
Plxnd1-/-
C
Migration front to midline distance (μm)
D
Vessel diameter (μm)
E
Number of branch points per field
F
Number of sprouts per field
Control
Sema3e-/-
Plxnd1-/-

Figure S4. *Sema3e*$^{-/-}$ embryos show dilated lymphatic vessels in the dorsal skin

(A, B) Whole-mount confocal images of control, *Sema3e*$^{-/-}$, or *Plxnd1*$^{-/-}$ dorsal skin labeled for PECAM, Prox1, and VEGFR3 at E16.5. In the dorsal skin, VEGFR3^{+} lymphatic vessels migrate from the two sides toward the midline (white dotted lines). White lines represent examples of migration front to midline distance. Boxed areas are magnified in the right panels. (**B**) *Sema3e*$^{-/-}$ and *Plxnd1*$^{-/-}$ mice showed an excessive number of sprouts (white arrowheads). (**C-F**) Quantification of distance from the migration front to midline (white lines in (**A**)), vessel diameter, number of branch points and number of sprouts (five points were counted in each sample). Each dot represents a value obtained from one sample. All the data are presented as the means±SEM, and statistical analyses were performed using a one-way ANOVA between groups and post hoc multiple comparisons using Bonferroni's test. ** P<0.01, *** P<0.001, **** P<0.0001. Scale bars, 500 μm (**A left panel**), 100 μm **(A right panels)**, 50 μm **(B)**.

Figure S4, related to Figure 4 and 5

Figure S5

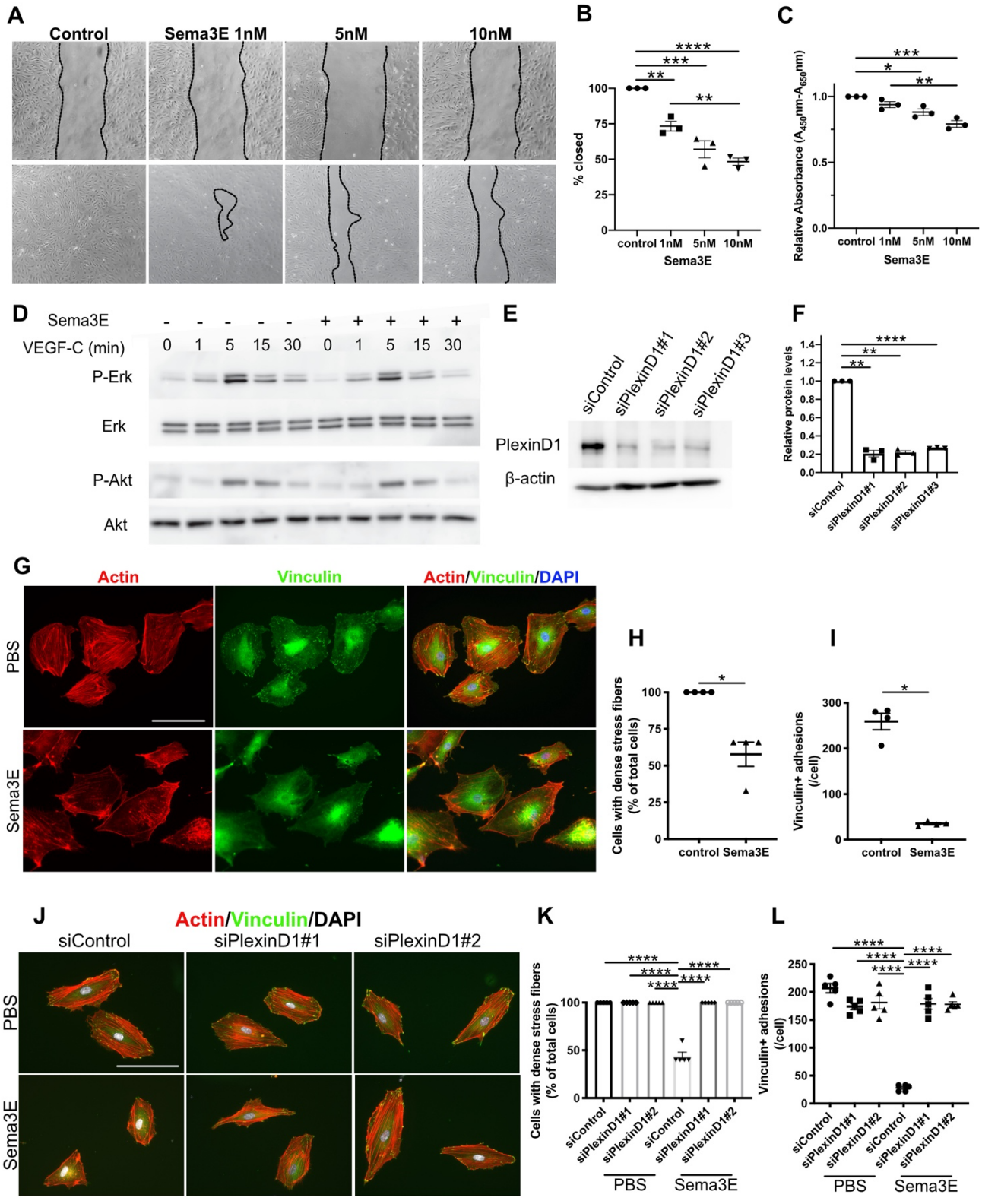
A
Control
Sema3E 1nM
5nM
10nM
B
% closed
control 1nM 5nM 10nM
Sema3E
C
Relative Absorbance (A450nm-A650nm)
control 1nM 5nM 10nM
Sema3E
D
Sema3E
VEGF-C (min)
0 1 5 15 30 0 1 5 15 30
P-Erk
Erk
P-Akt
Akt
E
siControl
siPlexinD1#1
siPlexinD1#2
siPlexinD1#3
PlexinD1
β-actin
F
Relative protein levels
siControl
siPlexinD1#1
siPlexinD1#2
siPlexinD1#3
G
Actin
Vinculin
Actin/Vinculin/DAPI
PBS
Sema3E
H
Cells with dense stress fibers (% of total cells)
control Sema3E
I
Vinculin+ adhesions (/cell)
control Sema3E
J
Actin/Vinculin/DAPI
siControl
siPlexinD1#1
siPlexinD1#2
PBS
Sema3E
K
Cells with dense stress fibers (% of total cells)
siControl
siPlexinD1#1
siPlexinD1#2
PBS
Sema3E
L
Vinculin+ adhesions (/cell)
siControl
siPlexinD1#1
siPlexinD1#2
PBS
Sema3E

Figure S5. Sema3E induces lymphatic endothelial cell retraction

(**A**) Wound healing assay in the absence or presence of recombinant Sema3E at indicated concentrations (1 nM, 5 nM and 10 nM). Percent closed area was quantified in (**B**) (n=3, biological replicates in all conditions). (**C**) MTT cell proliferation assay for the control or recombinant Sema3E treated HLECs. (**D**) LEC phosphorylation assay. HLECs exposed for 30 min to control medium or recombinant Sema3E (10 nM) were further cultured in the absence or presence of VEGF-C (200 ng/mL) for the indicated times, followed by lysis for western blotting of phosphorylated Akt (P-Akt), total Akt, phosphorylated Erk (P-Erk), and total Erk (n=5, biological replicates in all conditions). (**E, F**) Confirmation of PlexinD1 knockdown by western blotting with PlexinD1 antibody. Stealth siRNAs targeting three different regions of the PlexinD1 transcript. HLECs exposed to control or siPlexinD1 were further cultured for 72 h, followed by lysis for western blotting of PlexinD1 (n=3, biological replicates in all conditions). (**G**) HLECs were exposed to 10 nM recombinant Sema3E or PBS for 1 h and subsequently stained for F-actin, vinculin and DAPI. Quantification of the percentage of HLECs displaying an absence of dense actin stress fibers (**H**) or vinculin positive focal adhesions (**I**) (n=4, biological replicates in all conditions; 3 cells were analyzed in all conditions). (**J**) HLECs were transfected with control siRNA or siPlexinD1 and cultured to 80% confluency. Cells were passaged and seeded at 15% confluency. The following day, HLECs were exposed to PBS or 10 nM Sema3E for 1 h and stained for F-actin, vinculin, and DAPI. Vinculin^{+} focal adhesions and cells with dense stress fibers were quantified in (**K, L**) (n=5, biological replicates in all conditions; 5 cells were counted in each conditions). All results are expressed as the means ± SEM, and statistical analyses were performed using a one-way ANOVA between groups, post hoc multiple comparisons, Bonferroni's test. * P<0.05, ** P<0.01, *** P<0.001, **** P<0.0001. Scale bars, 100 μm **(G, J)**.

Figure S5, related to Figure 6

Figure S6

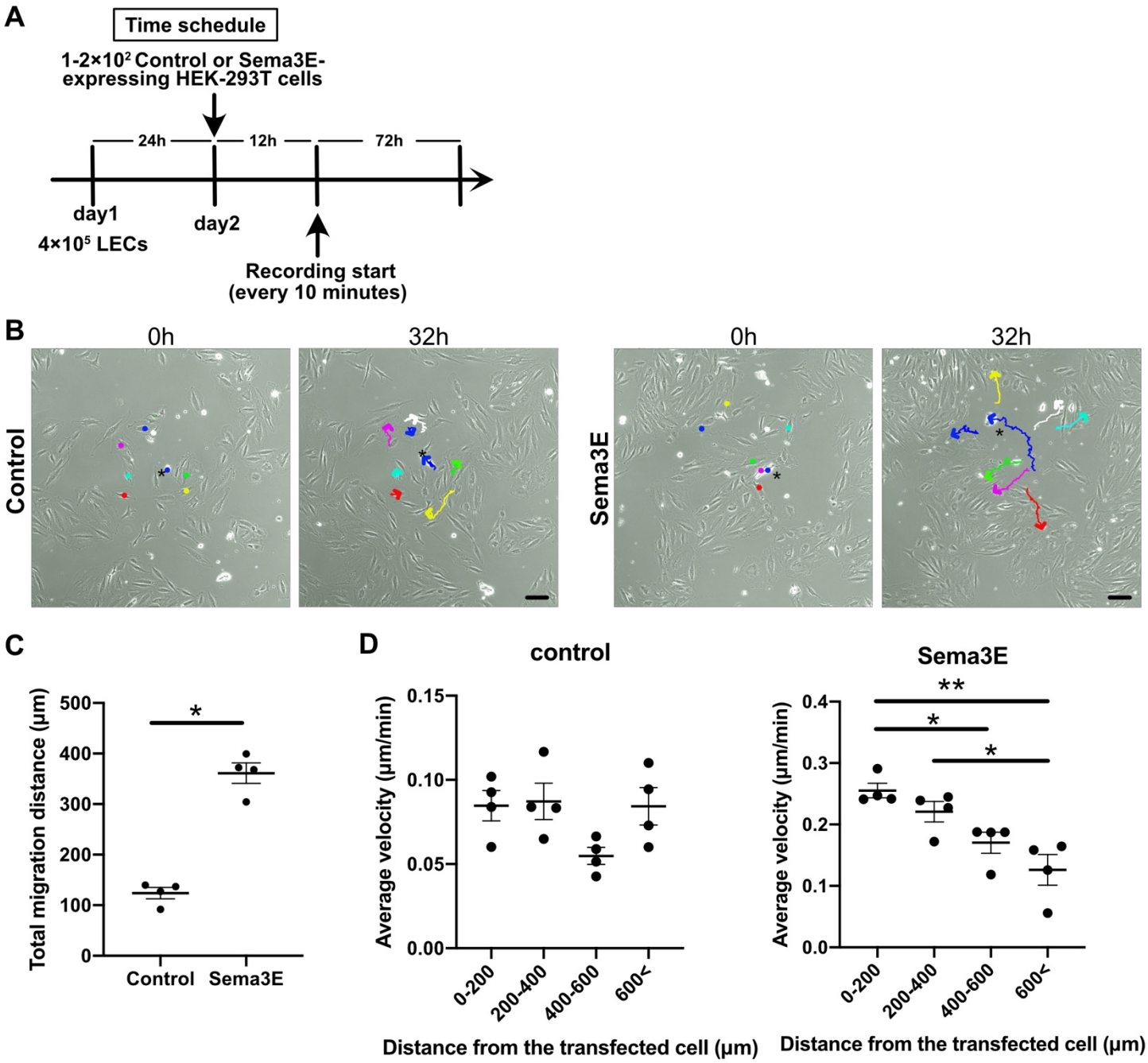
A
Time schedule
1-2×10² Control or Sema3E-expressing HEK-293T cells
24h
12h
72h
day1
4×10⁵ LECs
day2
Recording start
(every 10 minutes)
B
0h
32h
Control
Sema3E
C
Total migration distance (μm)
Control
Sema3E
D
control
Sema3E
Average velocity (μm/min)
0-200
200-400
400-600
600<
Distance from the transfected cell (μm)

Figure S6. Time-lapse imaging of the repelling effect of Sema3E-expressing cells on lymphatic endothelial cells

(**A**) Time schedule for the time-lapse imaging. (**B**) Control HEK-293T cells transfected with pFLAG-T2A-EGFP vectors (control) or HEK-293T cells transfected with pFLAG-Sema3E-T2A-EGFP (Sema3E) were seeded on top of HLECs and incubated for an additional 72 h. Tracks representing the migration paths of individual HLECs incubated for 32 h. Live-images were captured every 10 min. (**C, D**) Quantification of total length and average velocity in each condition (n=4, biological replicates in all conditions; 5-8 cells were tracked in each condition). All results are expressed as the means ± SEM, and statistical analyses were performed using a one-way ANOVA between groups, post hoc multiple comparisons, Bonferroni's test. * $P<0.05$, ** $P<0.01$. Scale bars, 100 μm **(B)**.

Figure S6, related to Figure 6

Figure S7

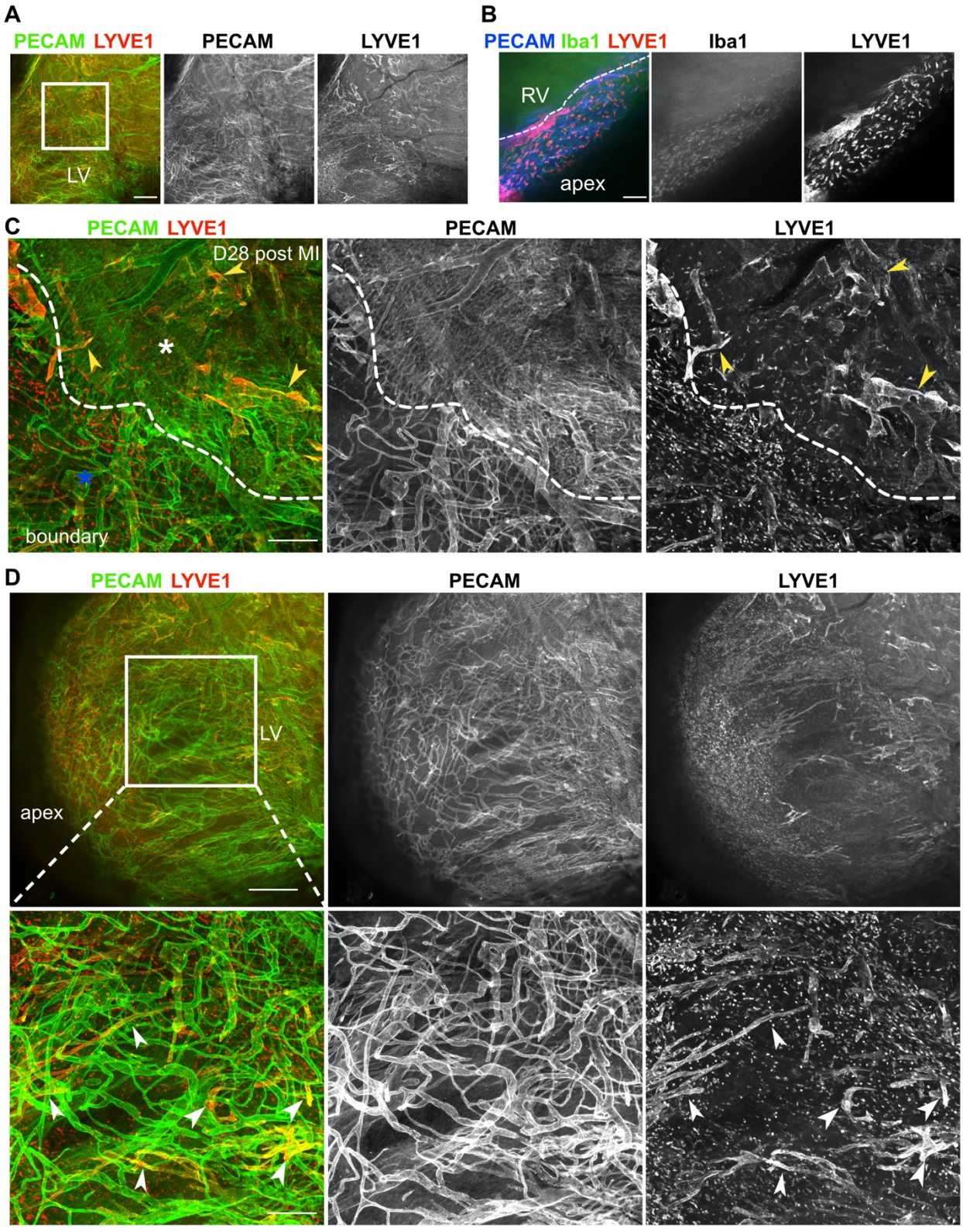
A
PECAM LYVE1
PECAM
LYVE1
LV
B
PECAM Iba1 LYVE1
Iba1
LYVE1
RV
apex
C
PECAM LYVE1
PECAM
LYVE1
D28 post MI
boundary
D
PECAM LYVE1
PECAM
LYVE1
LV
apex

Figure S7. Myocardial infarction induces substantial cardiac lymphangiogenesis and vascular remodeling

(A, C, D) Whole-mount confocal images of infarcted hearts stained for PECAM and LYVE1 on day 28 after MI. **(B)** $LYVE1^+$ cells colocalized with the macrophage marker Iba1 in the infarction area (white dotted line represents the boundary between the infarcted area and the non-infarcted area). **(C)** Boxed areas in **(A)** are magnified in **(C)**. White dotted lines represent the boundary between the infarcted area (blue asterisk) and the non-infarcted area (white asterisk). $LYVE1^+$ reactive lymphangiogenesis was observed in the non-infarcted area (yellow arrowheads). In contrast, $LYVE1^+$ macrophage infiltration was observed in the infarcted area. **(D)** A substantial number of $LYVE1^+$ macrophages had migrated into the infarcted area, and weak lymphangiogenesis was observed (white arrowheads). LV, left ventricle; RV, right ventricle; MI, myocardial infarction. Scale bars, 500 μm **(A, B and D top panels)**, 100 μm **(C and D bottom panels)**.

Figure S7, related to Figure 7

Figure S8

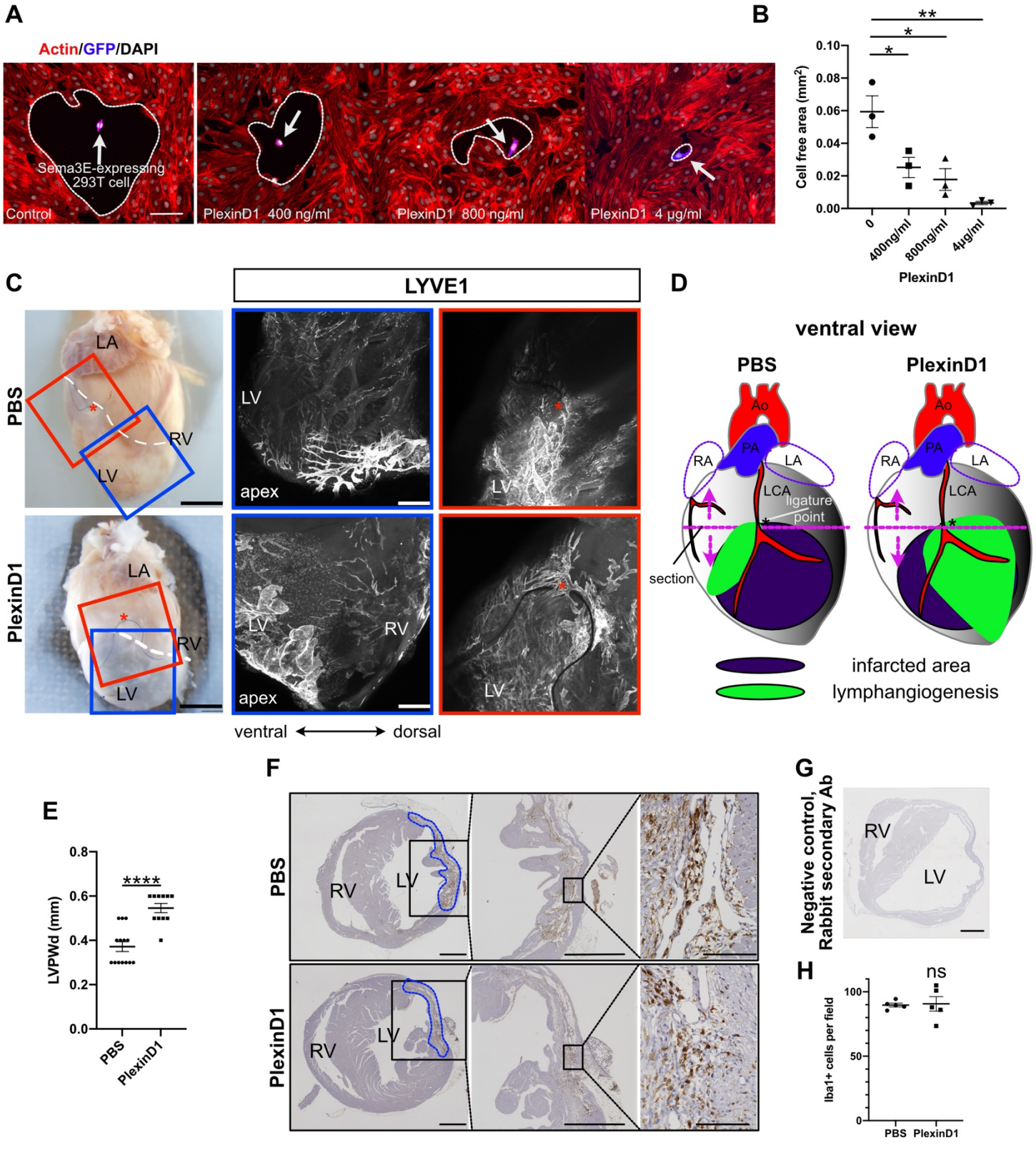
A
Actin/GFP/DAPI
Sema3E-expressing 293T cell
Control
PlexinD1 400 ng/ml
PlexinD1 800 ng/ml
PlexinD1 4 µg/ml
B
Cell free area (mm²)
0.10
0.08
0.06
0.04
0.02
0.00
0
400ng/ml
800ng/ml
4µg/ml
PlexinD1
C
LYVE1
PBS
PlexinD1
LA
RV
LV
apex
ventral ⟷ dorsal
D
ventral view
PBS
PlexinD1
Ao
PA
RA
LA
LCA
ligature point
section
infarcted area
lymphangiogenesis
E
LVPWd (mm)
0.8
0.6
0.4
0.2
0.0
****
PBS
PlexinD1
F
PBS
PlexinD1
RV
LV
G
Negative control, Rabbit secondary Ab
RV
LV
H
Iba1+ cells per field
100
50
0
ns
PBS
PlexinD1

Figure S8. Inhibition of Sema3E-PlexinD1 signaling stimulates angiogenesis and lymphangiogenesis

(A) LEC repulsive assay in the absence or presence of recombinant PlexinD1 at the indicated concentrations (400 ng/mL, 800 ng/mL, and 4 μg/mL). White dotted lines represent LEC free area and white arrows represent Sema3E-expressing HEK-293T cells. LEC free area was quantified in (**B**) (n=3, biological replicates in all conditions; 5-7 regions were counted in each condition). **(C)** Gross appearance and whole-mount confocal images of hearts treated with PBS or recombinant PlexinD1 (PlexinD1), stained for LYVE1 28 days after MI (red asterisks indicate the ligature suture points and white dotted lines represent the boundary between the infarcted area and non-infarcted area). Boxed areas in the left panels are magnified in the right panels. The $LYVE1^+$ lymphatic vessel area is schematically presented in **(D)**. (**E**) Evaluation of left ventricle posterior thickness at diastole (LVPWd). **(F, G)** Paraffin sections obtained from PBS- or recombinant PlexinD1-treated (PlexinD1) MI mice, immunostained for Iba1 or rabbit secondary antibody as a negative control. Blue dotted areas represent infarcted regions **(F).** The number of $Iba1^+$ macrophages was quantified in (**H**). LA, left atrium; RA, right atrium; LV, left ventricle; RV, right ventricle; MI, myocardial infarction; Ab, antibody. Each dot represents a value obtained from one sample. All results are expressed as the means ± SEM, and statistical analyses were performed using a one-way ANOVA between groups, and post hoc multiple comparisons using Bonferroni's test (**B**), or non-parametric Mann-Whitney's *u*-test (**H**). ns, $P \geq 0.05$, * $P<0.05$, ** $P<0.01$, **** $P<0.0001$. Scale bars, 2 mm (**C left panels**), 1 mm (**F left and middle panels**), 500 μm (**C middle panels**), 100 μm (**A**, **F right panels**).

Figure S8, related to Figure 7

TRANSPARENT METHODS

Mouse strains

The following mouse strains were employed: *Sema3e*$^{-/-}$ and *Plxnd1*$^{-/-}$ mice(Gu et al., 2005). *Sema3e*$^{+/+}$ and *Sema3e*$^{+/-}$ mice were used as controls; similarly, for *the Plxnd1* genotypes. The genotypes were determined by PCR using tail-tip or amnion DNA, and the specific primers are listed in Table 1. The mice were housed in an environmentally controlled room at 23±2°C, with a relative humidity of 50%–60% under a 12-h light:12-h dark cycle. The embryonic stages were determined by timed mating; the day the plug was observed was designated embryonic day (E) 0.5. Both female and male animals at E11.5 to E18.5 and postnatal day 7 were randomly subjected to the experiments and there was no difference in experimental results due to sex differences. All animal experiments were approved by the University of Tokyo and Tokyo Women's Medical University Animal Care and Use Committee and were performed in accordance with institutional guidelines.

Immunohistochemistry, histology, confocal imaging, and quantification

For histological analyses, hearts and embryos were collected, fixed with 4% paraformaldehyde (PFA), stored in PBS, embedded in paraffin (Kanto Chemical, Tokyo, Japan) or OCT (Sakura Finetek). Paraffin sections (4 μm) were stained with hematoxylin (Merck) and eosin (Kanto Chemical, Tokyo, Japan). Immunofluorescence staining of 4-μm paraffin or 16-μm frozen sections was performed using primary antibodies against CD31 (553370, BD Pharmingen, 1:50), Prox1 (11-002, AngioBio, 1:200), Prox1 (AF2727, R&D Systems, 1:200), LYVE1 (AF2125, R&D Systems, 1:50), VEGFR-3 (AF743, R&D Systems, 1:50), GFP (GF090R, Nacalai Tesque, 1:1000), GFP (GFP-RB-AF2020, FRL, 1:250), PlexinD1 (AF4160, R&D Systems, 1:100), vinculin (V9131, Merck, 1:200), endomucin (14-5851-85, eBioscience, 1:100), and Iba1 (019-19741, WAKO, 1:500). Alexa Fluor-conjugated secondary antibodies (Abcam, 1:200) were subsequently applied. The same protocol was utilized for whole-mounted hearts and embryos, but the primary and secondary antibody incubations were extended to two nights. Whole-mount 3,39-diaminobenzidine (DAB) staining was performed on embryonic and postnatal hearts using the Vectastain ABC System (Vector Laboratories). Images of the immunofluorescence staining were captured using a Nikon C2 confocal microscope. Maximum intensity z-projections of whole or sectioned hearts or skin were acquired using both the tiling and z-stack functions. The thickness of the z-projections was 10 μm for whole and 1 or 2 μm for sectioned samples. DAB staining was observed under a Keyence BZ-X700 microscope. All images were processed using ImageJ and Nikon NIS Elements software. Vessel areas were calculated using AngioTool (Zudaire et al., 2011).

Cryosection *in situ* hybridization was performed as previously described (Asai et al., 2010). The *Sema3e* probes were kindly gifted by Dr. Akiyoshi Uemura. The images were observed under a Keyence BZ-X700 microscope.

Wound healing assay

LECs (cc-2810, Lonza) were grown to confluence in EGM2 medium (cc-3162, Lonza) supplemented with 15% fetal bovine serum (FBS), and then shifted to LEC medium lacking growth factors and containing 0.5% FBS for 16 h. The confluent LECs were wounded using 1000-μL pipette tips. The remaining cells were washed twice with PBS to remove cell debris and then incubated in EGM2 medium supplemented with 15% FBS with PBS or Sema3E (3239-S3, R&D) for an additional 48 h. The images were observed under a Keyence BZ-X700 microscope, and the wound size was evaluated using NIH ImageJ.

LEC proliferation assays

LECs were seeded (5×10^4 cells/well) in 0.2% gelatin-coated 96-well plates and incubated for 24 h in EGM2 medium supplemented with 15% FBS. Then, the medium and/or Sema3E was added and incubated for an additional 48 h. The number of cells was determined using Cell Count Kit-8 (Doujindo, Kumamoto, Japan) and measured using a fluorescence spectrometer equipped with a microplate reader.

Phosphorylation assay

LECs were grown to confluence in growth medium and then shifted to medium lacking growth factors and containing 0.5% FBS for 16 h. Then, the cells were incubated with PBS or Sema3E (10 nM) for 2 h, followed by stimulation with VEGF-C (200 ng/mL). ERK1/2 and AKT phosphorylation was determined by western blotting.

Generation of expression vectors

To generate the pFLAG-T2A-EGFP vector, sequences corresponding to the picornavirus T2A and enhanced green fluorescent protein (EGFP) were inserted into the multiple-cloning site (MCS) of pFLAG-CMV2 (Sigma). The sequence for human Sema3E was also inserted into the MCS located before T2A of pFLAG-T2A-EGFP to generate pFLAG-Sema3E-T2A-EGFP. The constructs were verified by sequencing.

siRNA transfection

LECs were seeded in 0.2% gelatin-coated 6-well dishes at a concentration of 9×10^5 cells/well

in EGM2 medium supplemented with 15% FBS. The following day, cells were transfected with siControl (Invitrogen, medium GC duplex, 462001) or siPlexinD1 (Invitrogen, HS118222-4) using Lipofectamine RNAiMax transfection reagent (Invitrogen, 13778150) according to the manufacturer's instructions. The efficiency of siPlexinD1 was determined by western blotting. The sequences of siRNAs are shown in Table 2.

LEC repulsive assays

HLECs were cultured to 30-40% confluency. The following day, up to 2×10^2 HEK-293T cells transfected with pFLAG-T2A-EGFP or pFLAG-Sema3E-T2A-EGFP were seeded on top of LECs and incubated for an additional 48 h. For actin staining, cells were fixed with 4% PFA and incubated with Acti-stain 555 fluorescent phalloidin (Cytoskeleton) and GFP antibody (Nacalai Tesque), followed by incubation with secondary antibodies for GFP and DAPI for nuclear staining. Untreated LECs were used for time-lapse images, which were obtained every 10 min to 72 h using a confocal laser-scanning microscope (FluoView FV10i, Olympus). The obtained images were processed with FLUOVIEW (Olympus) and NIH ImageJ.

LEC spheroid sprouting assay

LECs were seeded in 0.2% gelatin-coated 6-well dishes at a concentration of 8×10^5 cells/well in EGM2 medium supplemented with 15% FBS. The following day, 1.2×10^6 LECs were mixed with EGM2 medium containing 0.24% methylcellulose (Sigma) and allowed to aggregate in round-bottom 96-well plates for 12 to 24 h (3000 cells per spheroids). The spheroids were subsequently embedded in type1 collagen (Nitta Gelatin, Osaka, Japan) and incubated for an additional 48 h. Then, spheroids were fixed in 4% PFA and incubated with fluorescent-labeled phalloidin (Cytoskeleton) and GFP antibody (Nacalai Tesque), followed by incubation with secondary antibody for GFP and DAPI for nuclear staining. Images were observed under a Keyence BZ-X700 microscope.

Murine cardiac injury model

Eight to twelve-week-old C57BL/6N male mice, weighing 22–27 g, underwent surgery. The mice were anesthetized with pentobarbital at 30 mg/kg for induction and 1.5-4.0% isoflurane for maintenance and were placed under assisted external ventilation after tracheal intubation. Cardiac injury was induced via permanent ligation of the left descending artery (LAD) at the medial location of the heart using a 10-0 ligature, and ST changes in the limb lead were monitored. Then, mice were randomly allocated to groups that received intraperitoneal injections of 0.1 μg/g recombinant PlexinD1 (4160-PD, R&D Systems) and PBS as a control.

Further injections were administered on days 2, 3, 4, and 6 post-surgery. The experimenters were double blinded to treatment and control assignments. The sample size was estimated using G*power (http://www.gpower.hhu.de/), and mice that died within 30 min of surgery were excluded from analyses as death due to surgery. Mice hearts were collected at 28 days post-MI and were either sectioned for histology and immunofluorescence staining or prepared for protein extraction. The mice were housed and maintained in a controlled environment.

Echocardiography

Echocardiography was performed in mice sedated with isoflurane, as previously described (Matsuura et al., 2009). Transthoracic echocardiography was performed using a Nemio 35 ultrasound system (Toshiba), with a 12-MHz imaging transducer, and the heart rate was maintained at approximately 500 bpm by adjusting the concentration of isoflurane to minimize data deviations during cardiac function measurements.

Western blotting

Total protein extract was obtained by lysing cells and the injured left ventricles of the MI hearts in RIPA buffer [150 mM NaCl, 0.1% Triton X-100, 0.5% Sodium deoxycholate, 0.1% SDS, 50 mM Tris-HCl (pH 7.6) supplemented with 25 mM NaF, 1 mM Na3VO4 and protein inhibitor cocktail (11873580001, Roche)]. Protein concentrations were quantified using DC protein assay kits (Bio-Rad). After equal amounts of proteins were loaded and separated via SDS–PAGE, the proteins were transferred to PVDF membranes (Immobilon-P, Millipore), blocked with 0.3% milk/TBST and incubated with primary antibodies against Sema3E (ab112886, Abcam, 1:10,000), VEGFR3 (AF743, R&D Systems, 1:5,000), β-Actin (sc-47778, Santa Cruz Biotechnology, 1:20,000), HPRT (GTX113466, GeneTex, 1:2,000), phospho-Erk (9106, Cell Signaling Technology, 1:1000), phospho-Akt (9271, Cell Signaling Technology, 1:1000), Akt (9272, Cell Signaling Technology, 1:1000), Erk (9102, Cell Signaling Technology, 1:1000), or PlexinD1 (AF4160, R&D Systems, 1:2,000) overnight at 4 °C. Then, membranes were incubated with horseradish peroxidase (HRP)-conjugated secondary antibodies (ab97110 or ab6721, Abcam, 1:5,000) for 1 h at room temperature. The proteins were detected using an ImageQuant LAS 4000 instrument (GE Healthcare).

Histological assessment of fibrosis

Serial 4 μm transverse paraffin sections of MI hearts were stained with Masson's trichrome solution and images were captured using a Keyence BZ-X700 microscope to quantify cardiac fibrosis. Using ImageJ software, the extent of fibrosis in sections was quantified as the relative

area of positive Masson's trichrome-stained area (blue fibrosis) normalized to the total section area.

Statistical analysis

Data are presented as the mean ± standard error of the mean (SEM). One-way analysis of variance (ANOVA) followed by Bonferroni's test was applied to multiple-group comparisons. Mann-Whitney's *u*-tests were applied to two-group comparisons. *P*-values less than 0.05 were considered statistically significant.

REFERENCES

Asai, R., Kurihara, Y., Fujisawa, K., Sato, T., Kawamura, Y., Kokubo, H., Tonami, K., Nishiyama, K., Uchijima, Y., Miyagawa-Tomita, S., Kurihara, H., 2010. Endothelin receptor type A expression defines a distinct cardiac subdomain within the heart field and is later implicated in chamber myocardium formation. Dev Camb Engl 137, 3823–33. https://doi.org/10.1242/dev.054015

Gu, C., Yoshida, Y., Livet, J., Reimert, D.V., Mann, F., Merte, J., Henderson, C.E., Jessell, T.M., Kolodkin, A.L., Ginty, D.D., 2005. Semaphorin 3E and Plexin-D1 Control Vascular Pattern Independently of Neuropilins. Science 307, 265–268. https://doi.org/10.1126/science.1105416

Matsuura, K., Honda, A., Nagai, T., Fukushima, N., Iwanaga, K., Tokunaga, M., Shimizu, T., Okano, T., Kasanuki, H., Hagiwara, N., Komuro, I., 2009. Transplantation of cardiac progenitor cells ameliorates cardiac dysfunction after myocardial infarction in mice. J Clin Invest 119, 2204–17. https://doi.org/10.1172/jci37456

Zudaire, E., Gambardella, L., Kurcz, C., Vermeren, S., 2011. A Computational Tool for Quantitative Analysis of Vascular Networks. Plos One 6, e27385. https://doi.org/10.1371/journal.pone.0027385

	Forward(5'-3')	Reverse(5'-3')
Sema3E KO	GACAGAAAGGCTTAGCGGATC	CTTGCTCACCATGGTGCGTG
Sema3E WT	GACAGAAAGGCTTAGCGGATC	GGTTCGCCGAGTGACCTG
PlxnD1 KO	ATGGTGAGCAAGGGCGAGGA	TTACTTGTACAGCTCGTCCA
PlxnD1 WT	ACCGCAGAACCGGTCACCGTGTT	GGTTAAGGTCGAAGGTGAAGAGCTT

Table 1. Primers used for genotyping.

Table 1, related to Figure1-5

	(5'-3')
siPlexinD1#1	GGAGGCUUCUCAAGAUCAACCUGAA
siPlexinD1#2	UGUUCCCGCUCAGCCUCCAACUAAA
siPlexinD1#3	GGGAAUUAGCUUGUUCUCCUCACUA

Table 2. The sequences of siPlexinD1

Table 2, related to Figure 6